A FUZZY MODELING OF ACTIVE MAGNETIC BEARING SYSTEM AND SLIDING MODE CONTROL WITH ROBUST HYPERPLANE USING μ-SYNTHESIS THEORY

Youzhi Xu
Precision Division,Ebara Densan Co.,Ltd, Fujisawa, 251-8521 Japan
xu@ed.ebara.co.jp
Kenzo Nonami
Dept. of Electronics and Mechanical Eng.,Chiba Univ.,Chiba, 263-8522 Japan
nonami@meneth.tm.chiba-u.ac.jp

ABSTRACT
The aim of this paper is to realize a sliding mode control system using robust hyperplane based on fuzzy model[1] for active magnetic bearing (AMB) system with gyroscopic rotation. A fuzzy model of AMB system is built from the input and output data of the actual turbo-molecular pump by using fuzzy neural network(FNN)[2]. The sliding mode controller has a switching hyperplane using μ -synthesis theory which has a powerful robustness and can suppress spillover phenomena. The ultra high-speed operation test of the actual turbo-molecular pump has been done by using the proposed controller. The good experimental results have been obtained. Therefore, it has been clarified that the proposed scheme is very useful strategy for AMB system.

INTRODUCTION
A lot of research[3]-[5]of the application of robust control theory in the AMB digital control are reported. Here, the mathematical model of the AMB system is already-known in these researches. However, There are a lot of cases that this mathematical model cannot be derived in the real system.
In this paper, the AMB system which the mathematical model is not obtained is identified by using the FNN technology. And, the sliding mode control method which has robust hyperplane based on the μ-synthesis theory is proposed for this fuzzy model of the AMB identified.
First of all, in order to design robust hyperplane using μ -synthesis theory, the controlled system is shown by the equation of the canonical form in this report. The modeling is done as a two output system. Next, a structural perturbation block which includes the actual parameter is made from the obtained fuzzy model, and the AMB control system by the sliding mode control which has robust hyperplane using μ -synthesis theory is designed. In this hyperplane, the robust stability and the robust performance to two or more structural uncertainties are possessed. And, the control system was mounted on the digital control machine which used DSP, and the levitation and the rotation experiment with a real machine were done with the turbo-molecular pump(TMP) which reached the rated operation 45000 rpm. Moreover, in order to verify the robust control performance, the experiments using real machines of the AMB system with a different parameter were done. As a result, the effectiveness of the technique proposed with this paper was proven.

MODELING
A Basic Structure of Five Axes AMB
FIGURE 1 shows a basic structure of five axes AMB. In this research, to give priority to practical use and easily of design, five axes are assumed to be an independent AMB model of one mass respectively.

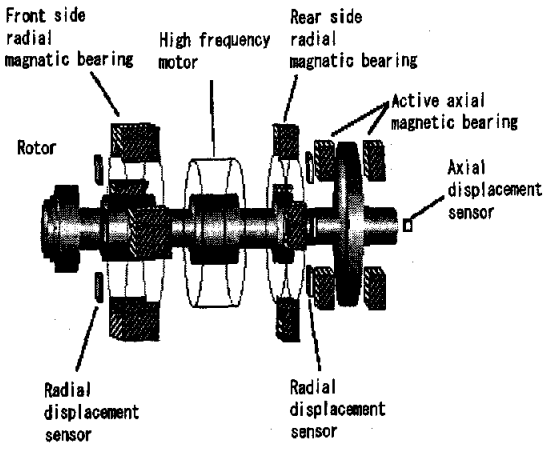

FIGURE 1: Active magnetic bearing system

Fuzzy Model of AMB

A fuzzy model is a model described by the if-then form used by the reasoning method of the fuzzy control. If a dynamic input-output relation is shown by the difference equation, the consequent part becomes the dynamical model of the controlled system. In this research, the structure of a fuzzy model chooses the premise part input variable to be the rotor displacement(x_k) and the primary time difference of the rotor displacement(Δx_k) , and makes the consequent part input variable to be the rotor displacement(x_k) and the primary time difference of the rotor displacement(Δx_k) and manipulated variables(u_k). Moreover, we decide the consequent part output to be the rotor displacement(x_{k+1}) and the primary time difference of the rotor displacement(Δx_{k+1}) after one sampling. The fuzzy models are as follows:

$$L^1: if \quad x_k \; is \; small(A_{11}) \; and \; \Delta x_k \; is \; small(A_{12}) \quad then$$
$$x^1_{k+1} = a^1_{11}x_k + a^1_{12}\Delta x_k, \quad \Delta x^1_{k+1} = a^1_{21}x_k + a^1_{22}\Delta x_k + a^1_{23}u_k \tag{1}$$

$$L^2: if \quad x_k \; is \; small(A_{11}) \; and \; \Delta x_k \; is \; big(A_{22}) \quad then$$
$$x^2_{k+1} = a^2_{11}x_k + a^2_{12}\Delta x_k, \quad \Delta x^2_{k+1} = a^2_{21}x_k + a^2_{22}\Delta x_k + a^2_{23}u_k \tag{2}$$

$$L^3: if \quad x_k \; is \; big(A_{21}) \; and \; \Delta x_k \; is \; small(A_{12}) \quad then$$
$$x^3_{k+1} = a^3_{11}x_k + a^3_{12}\Delta x_k, \quad \Delta x^3_{k+1} = a^3_{21}x_k + a^3_{22}\Delta x_k + a^3_{23}u_k \tag{3}$$

$$L^4: if \quad x_k \; is \; big(A_{21}) \; and \; \Delta x_k \; is \; big(A_{22}) \quad then$$
$$x^4_{k+1} = a^4_{11}x_k + a^4_{12}\Delta x_k, \quad \Delta x^4_{k+1} = a^4_{21}x_k + a^4_{22}\Delta x_k + a^4_{23}u_k \tag{4}$$

Here, L^i is a rule of a fuzzy model. a^i_{11},a^i_{12},a^i_{21},a^i_{22},and a^i_{23} are the consequent part parameters of rules(i=1,2,3,4). $A_{j_1 1}$ and $A_{j_2 2}$ are the premise part membership functions(j_1,j_2=1,2). uk is manipulated variable.

Identification of Fuzzy Model

A fuzzy modeling is to identify various parameters of a fuzzy model of Eqs.(1)-(4) by using the input-output data of the controlled system. There is FNN technology in this fuzzy modeling most as an effective technique. This achieves calculations process of the fuzzy reasoning by the structure of the back propagation model of the neural network. In this research, we apply the FNN technology, and construct FNN to identify various parameters of Eq.(1). FIGURE 2 shows FNN structure.The premise part membership function is obtained from Eq.(5) and Eq.(6), and is corresponding to the output of the unit

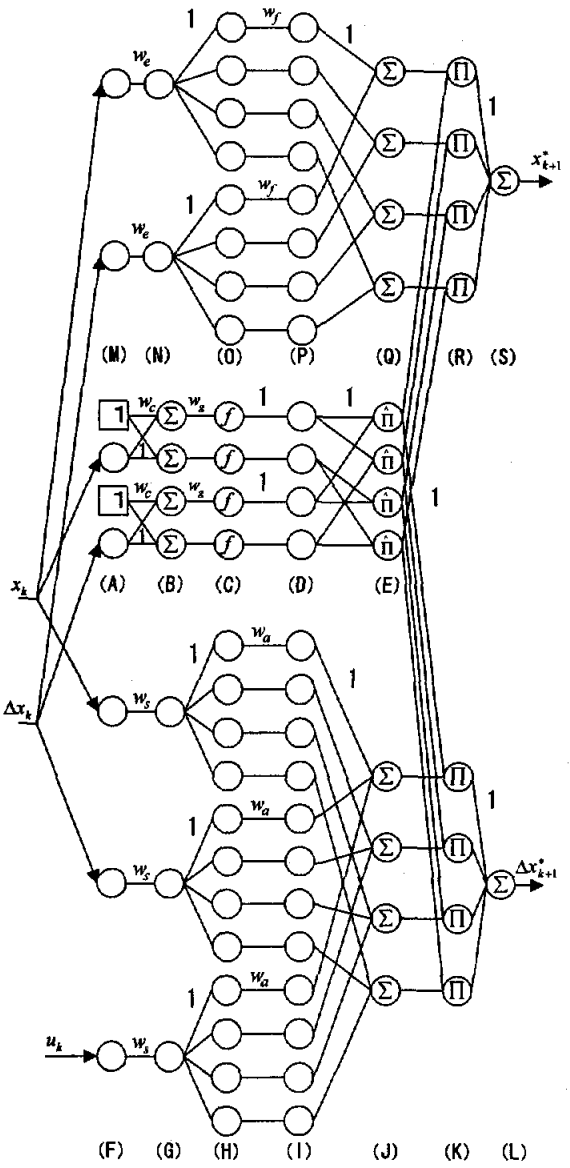

FIGURE 2: Structures of FNN

in the (C) layer.

$$f(x) = \frac{1}{1+\exp(-x)} \tag{5}$$

$$O^c_j = \frac{1}{1+\exp\{-w_g(x_j + w_c)\}} \tag{6}$$

Here, $x_j = x_k$、Δx_k. The weighting coefficients Wc and Wg are parameters which provide the center location and the inclination of the shigmoid function respectively. FIGURE 3 shows the shape of the premise part membership function. In the (E) layer, the input is the premise part adaptation μ_i , and the output is a value standardized by the sum total. They

are

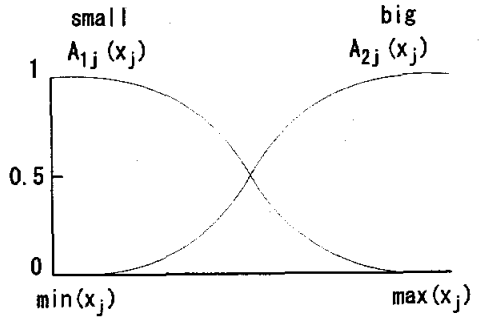

FIGURE 3: Membership Function

obtained from Eq.(7) and Eq.(8) respectively.

$$\mu_i = A_{j_1 1}(x_k) A_{j_2 2}(\Delta x_k) \tag{7}$$

$$\tilde{\mu}_i = \frac{\mu_i}{\sum_q \mu_q} \tag{8}$$

Moreover, the consequent part output(x^i_{k+1}) of the rule of the each fuzzy model shown by Eq.(9) is obtained from the output in the (Q) layer, and the consequent part output(Δx^i_{k+1}) of the rule of the each fuzzy model shown by Eq.(10) is obtained from the output in the (J) layer.

$$x^i_{k+1}(x_k, \Delta x_k) = a^i_{11} x_k + a^i_{12} \Delta x_k \tag{9}$$

$$\Delta x^i_{k+1}(x_k, \Delta x_k, u_k) = a^i_{21} x_k + a^i_{22} \Delta x_k + a^i_{23} u_k \tag{10}$$

Here, a^i_{11} and a^i_{12} are products of weighting coefficients We and Wf. a^i_{21}, a^i_{22}, and a^i_{23} are products of weighting coefficients Ws and Wa. For a certain input, the fuzzy reasoning value(x^*_{k+1}) is calculated like Eq.(11) in the (R) layer and the (S) layer, and the fuzzy reasoning value(Δx^*_{k+1}) is calculated like Eq.(12) in the (K) layer and the (L) layer.

$$x^*_{k+1} = \sum_{i=1}^{4} \tilde{\mu}_i x^i_{k+1}(x_k, \Delta x_k) \tag{11}$$

$$\Delta x^*_{k+1} = \sum_{i=1}^{4} \tilde{\mu}_i \Delta x^i_{k+1}(x_k, \Delta x_k, u_k) \tag{12}$$

The weighting coefficient is updated by the back propagation method. A lot of the methods are used for the study method. The output error performance function is defined like Eqs.(13)- (16).

$$E_k = \frac{1}{2}(x_{k+1} - x^*_{k+1})^2 \tag{13}$$

$$E = \sum_{k=1}^{K} E_k \tag{14}$$

$$EE_k = \frac{1}{2}(\Delta x_{k+1} - \Delta x^*_{k+1})^2 \tag{15}$$

$$EE = \sum_{k=1}^{K} EE_k \tag{16}$$

The weighting coefficient is updated by Eqs.(17)-(19).

$$\delta^{1(n)}_j = -\frac{\partial E_k}{\partial I^{(n)}_j} \tag{17}$$

$$\delta^{2(n)}_j = -\frac{\partial EE_k}{\partial I^{(n)}_j} \tag{18}$$

$$w^{(n)}_{ji}(m+1) = w^{(n)}_{ji}(m) + \eta^{(n)}_{ji} \delta^{l(n)}_j O^{(n-1)}_i \tag{19}$$

Here, $\delta_j^{l(n)}$ is a output error of n layer j unit, and it spreads from the output layer to the input layer in the opposite direction(l=1,2). $W_{ji}^{(n)}$ is the weighting coefficient between the n-1 layer and n layer . $\eta_{ji}^{(n)}$ is a study rate to $W_{ji}^{(n)}$. $I_j^{(n)}$ is the input of n layer j unit . $O_i^{(n-1)}$ is i unit output of the n-1 layer.

The collection, the selection, and the correction of the input-output data used to identify the model are very important in the modeling. In this research, the real levitation test of the TMP (The experiment machine No.1: 2.5kg in the mass of the rotor and rated speed 45000 rpm) which is the controlled system of this research is tested with a past, analog AMB controller. The model identification uses the input-output data obtained from this experiment.

DESIGN OF ROBUST HYPERPLANE

Introduction of State Equation

In this research, the consequent part of a fuzzy model of the AMB system are several linear relational expressions which show the dynamic characteristic of the controlled system like Eqs.(1)-(4). Here, an approximate common nominal parameter and structural width of the change are obtained from the parameter of the consequent part respectively as follows:

$$A_{11} = \frac{\max\_a_{11} + \min\_a_{11}}{2}, \quad \Delta A_{11} = \frac{\max\_a_{11} - \min\_a_{11}}{2} \tag{20}$$

$$A_{12}=\frac{\max\_a_{12}+\min\_a_{12}}{2},\quad \Delta A_{12}=\frac{\max\_a_{12}-\min\_a_{12}}{2} \tag{21}$$

$$A_{21}=\frac{\max\_a_{21}+\min\_a_{21}}{2},\quad \Delta A_{21}=\frac{\max\_a_{21}-\min\_a_{21}}{2} \tag{22}$$

$$A_{22}=\frac{\max\_a_{22}+\min\_a_{22}}{2},\quad \Delta A_{22}=\frac{\max\_a_{22}-\min\_a_{22}}{2} \tag{23}$$

$$B_2=\frac{\max\_a_{23}+\min\_a_{23}}{2},\quad \Delta B_2=\frac{\max\_a_{23}-\min\_a_{23}}{2} \tag{24}$$

Here, $\max\_a_{ij}$ and $\min\_a_{ij}$ show the maximum value and the minimum value of $a_{ij}^{(n)}$ respectively (i=1,2;j=1,2,3;n=1,2,3,4). Moreover, these nominal parameters are obtained from the discrete system, and when a continuous system design method is used, it only has to convert the discrete system parameter into a continuous system parameter by MATLAB. Therefore, an approximate equation of state of the AMB to design the controller is decided like Eq.(25).

$$\begin{bmatrix}\dot{x}_1\\ \dot{x}_2\end{bmatrix}=\begin{bmatrix}A_{11}\ A_{12}\\ A_{21}\ A_{22}\end{bmatrix}\begin{bmatrix}x_1\\ x_2\end{bmatrix}+\begin{bmatrix}0\\ B_2\end{bmatrix}u \tag{25}$$

Hyperplane Design Using μ-Synthesis Theory

First of all, hyperplane with dynamics is defined like Eq.(26) in the system of Eq.(25).

$$\Psi=S(x_1)+x_2 \tag{26}$$

At this time, S(.) is the linear operator like Eq.(27).

$$\begin{aligned}\dot{z}&=Fz+Gx_1\\ S(x_1,z)&=Hz+Lx_1\end{aligned} \tag{27}$$

When the state is constrained on hyperplane ($\Psi=\dot{\Psi}=0$), the system of Eq.(25) is former made low-level of Eq.(28). At this time, x_2 is written by Eq.(29).

$$\begin{aligned}\dot{z}&=Fz+Gx_1\\ \dot{x}_1&=A_{11}x_1+A_{12}x_2\end{aligned} \tag{28}$$

$$\begin{aligned}x_2&=-S(x_1)\\ &=-Hz-Lx_1\end{aligned} \tag{29}$$

It is found that x_1 is the state and x_2 is the new input on hyperplane. Therefore, the block diagram of hyperplane when the μ-synthesis theory is used is given by FIGURE 4. Here, W_1 is used as a weighting function corresponding to the unmodeled dynamics, especially the uncertainty in the high frequency band. ΔA_{11} and ΔA_{12} are the weights of a structural uncertainty of nominal parameter A_{11} and A_{12}. They are decided by the width of the parameter variation of Eqs.(20) and (21) respectively. These are related to guarantee the robust stability. W_2 is a weighting

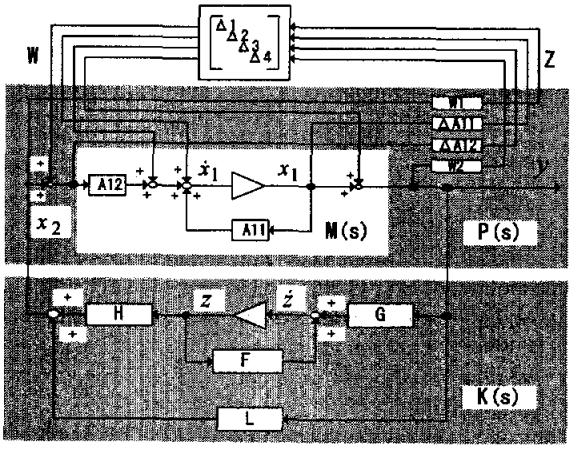

FIGURE 4: Block diagram of generalized plant

function used for nominal performance. M is the reduced order plant. P is the generalized plant including the weighting function. K is the compensator to stabilize the system on hyperplane. Therefore, the hyperplane design becomes to decide {F,G,H,L} of matrix K by the μ-synthesis theory. Moreover, the performance function of Inequality (30) is obtained for the system of FIGURE 4 in μ-synthesis theory. A left hand side of expression (31) means the structured singular value. To satisfy these two expressions both, compensator K is designed.

$$\left\|\begin{matrix}W_1(I+KM)^{-1}KM\\ \Delta A_{11}A_{12}^{-1}(I+KM)^{-1}M\\ \Delta A_{12}A_{12}^{-1}(I+KM)^{-1}KM\\ W_2(I+KM)^{-1}\end{matrix}\right\|_\infty<1 \tag{30}$$

$$\mu_\Delta(LFT(P,K))<1 \tag{31}$$

As an example, Eq.(32), Eq.(33), and FIGURE 5 show weighting function(W1 and W2) which is set by the try and error in the upper x direction. The dynamic characteristics of obtained compensator K become the low-pass filter like FIGURE 6.

$$w_1=\frac{2s+5}{s+1000} \tag{32}$$

$$w_2=\frac{0.0025s+25000}{s+5000} \tag{33}$$

There is a feature that this controller K does not control in high frequency band though the nonlinear sliding mode control input strongly works in low frequency range. It seems to be extremely effective to

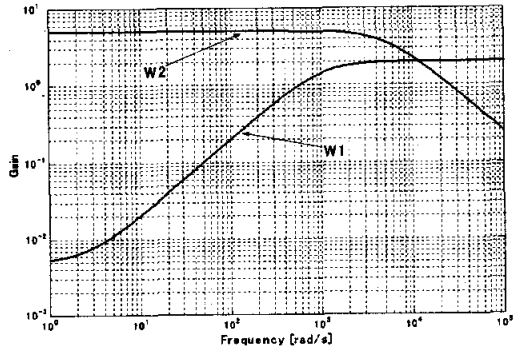

FIGURE 5: Gain plots of weighting functions

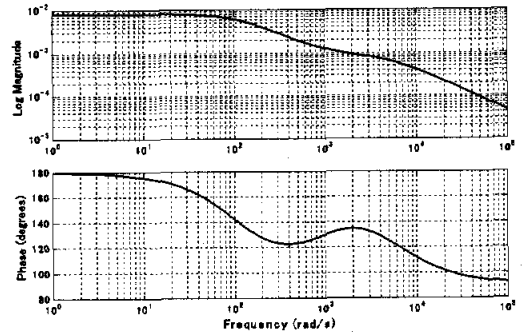

FIGURE 6: Frequency response of K

AMB system which has the ultra high-speed rotor like the TMP as the measures of the spillover, chattering, and high frequency noise.

DESIGN OF SLIDING MODE CONTROLLER

When the sliding mode exists, an equivalent control input in hyperplane can be expressed as Eq.(34) by using Eqs.(25), (28), and (29).

$$u_{eq} = -B_2^{-1}[HFz + (HG + LA_{11} + A_{21})x_1 + (LA_{12} + A_{22})x_2] \quad (34)$$

Next, the reaching condition or the variable structure control rule to constrain the state on hyperplane is derived. The candidate of the Lyapunov function is chosen by Eq.(35) as the switching function Ψ. The variable structure control rule is provided as Eq.(37).

$$V = \frac{1}{2}\Psi^2 \quad (35)$$

$$\begin{aligned}\dot{V} &= \Psi \cdot \dot{\Psi} \\ &= \Psi[HFz + (HG + LA_{11} + A_{21})x_1 + (LA_{12} + A_{22})x_2 + B_2 u] \\ &= B_2\Psi(u - u_{eq}) < 0\end{aligned} \quad (36)$$

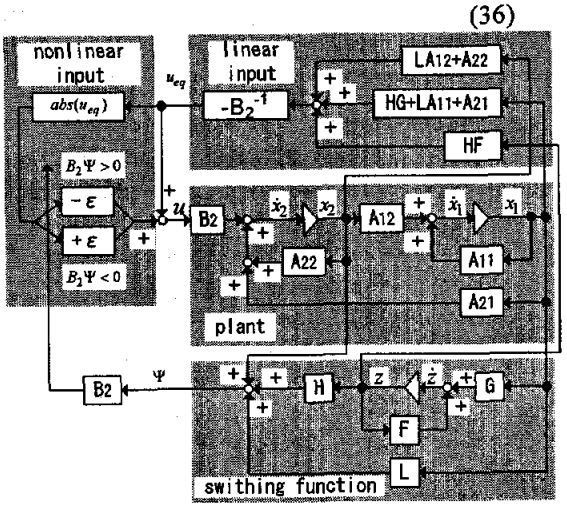

FIGURE 7: SMC with H_∞ robust hyperplane

$$u = \begin{cases} u_{eq} - \varepsilon|u_{eq}|, & B_2\Psi > 0 \\ u_{eq} + \varepsilon|u_{eq}|, & B_2\Psi < 0 \end{cases} \quad (37)$$

Here, ε is the positive number denotes switching width, and is decided by try and error with an judgement of the control performance and the value of the control input. Moreover, the block diagram of the sliding mode control system which has μ-robust hyperplane is finally shown in FIGURE 7.

EXPERIMENT

Experiment Method

The system shown in FIGURE 8 was composed for the experiment. The SMC control law is installed on DSP. The sampling time is 0.1 msec. The different experiment machines shown in Table 1 were used for the experiment. The first experiment machine is a controlled system used to design control system. The second experiment machine and the third experiment machine have the large change compared with the first experiment machine in the parameter. Thus, they are used to verify the robust performance of the control system.

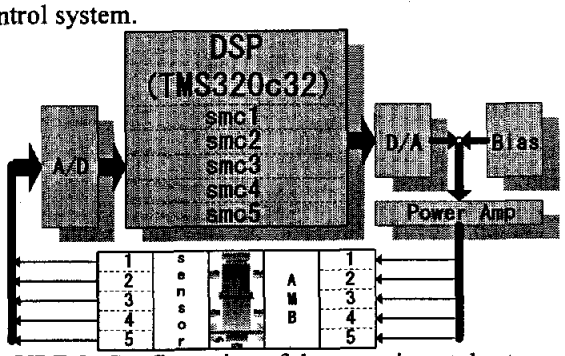

FIGURE 8: Configuration of the experimental setup

TABLE 1 Rotor specification of test rig

Test rig No.	Mass (kg)	Diameter (mm)	Length (mm)
1	2.5	37	224
2	8	52	257
3	9	52	276

Experiment Result

First of all, the real levitation and the rotation test were done with the first experiment machine. FIGURE 9 shows the time history response from arbitrary initial state to the stable levitation in the upper and lower x directions. It is found that the state of the stability is realized within 0.2 seconds from the figure, and the excellent control was achieved. Because the y direction obtained the same result as the x direction, these results were omitted here. Moreover, because the control of the z direction is easier than one of the x and the y directions, this result is also omitted here. FIGURE 10(a,b) is Lissajou's wave of the upper and lower directions at the levitated state respectively. The left hand side is three dimensional display, and the vertical direction indicates the time. The right hand side shows the orbits. FIGURE 10(c,d) is Lissajou's wave of the upper and lower directions at the rated rotation state(45000rpm) respectively. It is found that the diameter of the orbits are only several μm or less from this figure. FIGURE 11 shows the behavior of the upper x direction from the state of the stable levitation up to the operational speed as one example. Moreover, in order to verify the robust performance, the real levitation tests with the second machine (the operational speed 35000 rpm) and the third machine were done using the controller for the first machine. FIGURE 12(a,b) shows the time history response of the second machine and the 3rd machine from arbitrary initial state to the stable levitation in the upper and lower x directions. It is found that the state of the stability is realized within 0.5 seconds from the figure for both machines. In addition, the real rotation test up to the operational speed was done with the second machine. FIGURE 13(a,b,c,d) and FIGURE 14 show the results. FIGURE 13(a,b) is Lissajou's wave of the upper and lower directions at 0rpm state respectively. FIGURE 13(c,d) is Lissajou's wave of the upper and lower directions at 35000rpm state respectively. FIGURE 14 shows the behavior of the upper x direction from the state of the stable levitation to the operational speed as one example. It is found that the second machine with a large parameter variation achieved a high-speed rotation(35000rpm) from these figures. Moreover, the vibration is suppressed within several μm during the whole rotational speed.

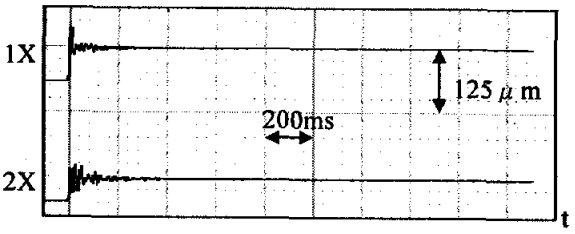

FIGURE 9: Time history response of test rig1 from initial state

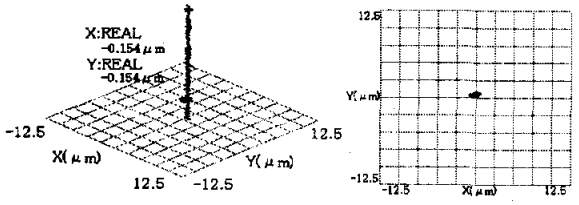

(a) Upper side of test rig1(0rpm)

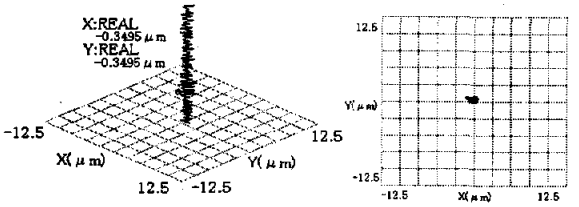

(b)Below side of test rig1(0rpm)

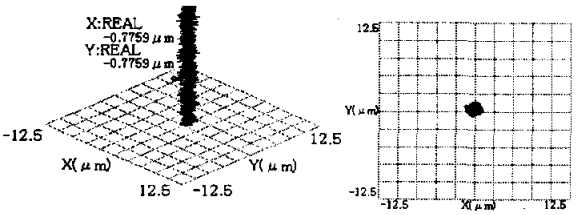

(c)Upper side of test rig1(45000rpm)

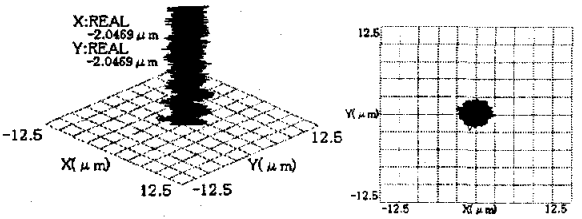

(d)Below side of test rig1(45000rpm)

FIGURE 10: 3-D orbit of shaft center

CONCLUSIONS

In this research, the AMB system was expressed by the fuzzy model, and the fuzzy modeling of the AMB was done by FNN. The sliding mode control method which has robust hyperplane based on the μ-synthesis theory is proposed for this fuzzy model. And, the experiment using the commercial use machine up to ultra high-speed rotation was done with TMP.

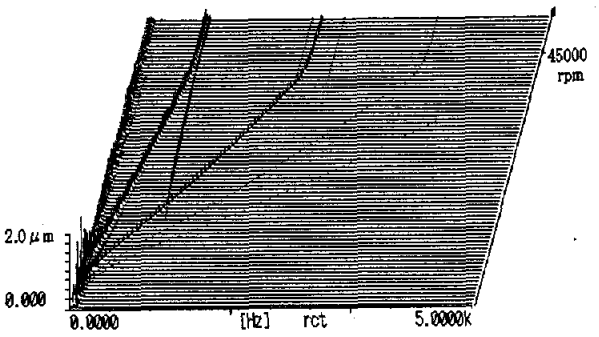

FIGURE 11: Water fall plots(1X of test rig1)

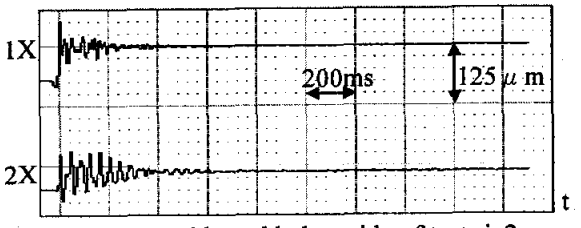

(a) Upper side and below side of test rig2

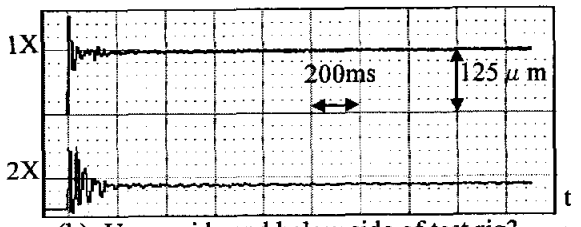

(b) Upper side and below side of test rig3

FIGURE 12: Time history response from initial state (X direction)

Moreover, in order to verify the robust performance, the experiments using the real machine with a different parameter were done. As these results, the effectiveness of the technique proposed with this paper was confirmed.

REFERENCES

1. T.Takagi, M.Sugeno, Fuzzy Identification of Systems and Its Applications to Modeling and Control, IEEE Trans.SMC,15-1, pp.116-132,1985.
2. S.Horikawa,T.Furubasi,Y.Utikawa, Compsition Methods and Learning Algorithms of Fuzzy Neural Network, Journal of Japan Society Fuzzy Theory and Systems , 4-5, pp.906-928,1992.
3. S.Sivrioglu, K.Nonami,Gain Scheduled Sliding Mode Control of Active Magnetic Bearing System with Gyroscopic Rotor, JSME, series C, 65-635, pp 2665-2671,1999.
4. S.Sivrioglu, K.Nonami,Gain Scheduled H_∞ Control of Active Magnetic Bearing Systems with Gyroscopic Effect, JSME,series C,63-610,pp1940-1947, 1997.

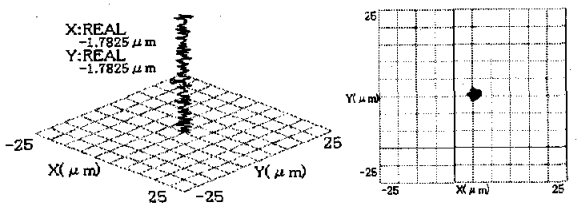

(a) Upper side of test rig2(0rpm)

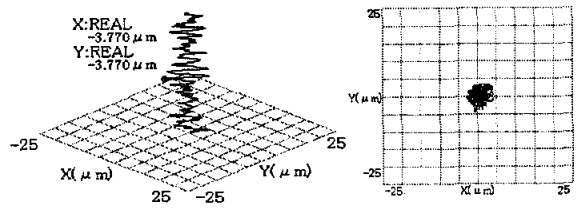

(b)Below side of test rig2(0rpm)

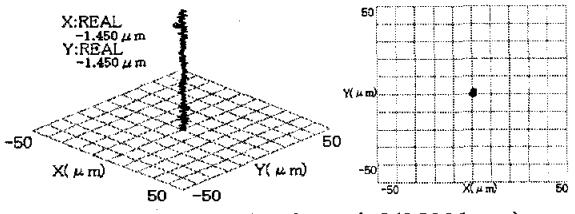

(c)Upper side of test rig2(35000rpm)

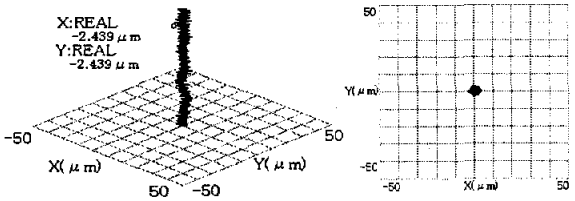

(d)Below side of test rig2(35000rpm)

FIGURE 13: 3-D orbit of shaft center

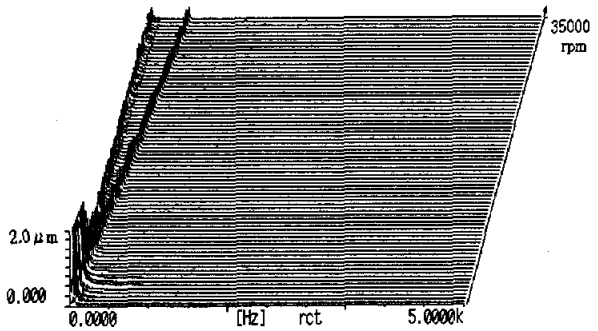

FIGURE 14: Water fall plots(1X of test rig2)

5. T.Itou, K.Nonami, μ -Synthesis of Flexible Rotor-Magnetic Bearing System, JSME, series C, 61-584, pp1437-1442, 1995.